ENERGY TRANSFER

Quantum coherence as a witness of vibronically hot energy transfer in bacterial reaction center

David Paleček,[1,2]* Petra Edlund,[3] Sebastian Westenhoff,[3] Donatas Zigmantas[1]†

Photosynthetic proteins have evolved over billions of years so as to undergo optimal energy transfer to the sites of charge separation. On the basis of spectroscopically detected quantum coherences, it has been suggested that this energy transfer is partially wavelike. This conclusion depends critically on the assignment of the coherences to the evolution of excitonic superpositions. We demonstrate that, for a bacterial reaction center protein, long-lived coherent spectroscopic oscillations, which bear canonical signatures of excitonic superpositions, are essentially vibrational excited-state coherences shifted to the ground state of the chromophores. We show that the appearance of these coherences arises from a release of electronic energy during energy transfer. Our results establish how energy migrates on vibrationally hot chromophores in the reaction center, and they call for a reexamination of claims of quantum energy transfer in photosynthesis.

INTRODUCTION

For efficient photosynthesis, energy migrates through large chromophore assemblies to the active site of charge generation. Although this transfer is generally downhill in energy, every energy transfer step must obey the law of energy conservation. This means that vibrational or environmental modes take up the excess energy of each transfer step. However, identification of these critical modes and their coupling to electronic transitions is difficult, because these processes are not readily observable in conjunction with energy transfer using current spectroscopic methods.

Following absorption of a short laser pulse, the electron cloud and atoms oscillate coherently across the molecules; electronic and vibrational coherences are established. Coupling to the environment (for example, to solvent molecules or a protein binding pocket) leads to dephasing of these coherences across the molecules. Vibrational wave packets have been observed in photosynthetic proteins using femtosecond transient absorption experiments in the visible and near-infrared spectral regions (*1*, *2*). In addition, polarization-resolved experiments provided early evidence for electronic coherences in photosynthetic proteins (*3*, *4*). The advent of two-dimensional electronic spectroscopy (2DES) opened a new avenue for studying electronic and vibrational coherences (*5*–*7*). The higher dimensionality of the data in these experiments leads to less spectral congestion, thereby enabling more detailed insight (*8*–*10*).

In the 2DES experiment, a sequence of three ultrashort laser pulses (with time delays t_1 and t_2 between them) excites the sample. A third-order polarization is induced in the sample, and the emitted signal field is detected with a fourth pulse at t_3 after the last excitation pulse. The evolution of the excited states is then resolved in the two-dimensional (2D) spectra relating excitation (ω_1) and detection (ω_3) frequencies, which are Fourier transform conjugates of the t_1 and t_3 time delays, respectively (*5*). Coherences between states are detected as oscillatory signals along t_2. It is very challenging to distinguish between electronic and vibrational origins of the coherences, but polarization-resolved 2DES (*11*–*14*), an additional Fourier transform over population time t_2 (*15*, *16*), and theoretical analysis (*17*, *18*) have been developed to this end.

The first reports on 2D electronic spectra of light-harvesting proteins created excitement, because it was concluded that electronic coherences live for more than a picosecond (*6*, *12*, *19*). This would suggest that energy could migrate wavelike through the photosynthetic proteins. This far-reaching conclusion relies on the assignment of the observed oscillations to electronic coherences. From the outset, survival of electronic coherences in proteins for picoseconds seems questionable, because the environment and intramolecular vibrations readily induce fluctuation of electronic transitions on a femtosecond time scale. Thus, electronic coherences should decay much faster than vibrational coherences, which typically dephase within a couple of picoseconds.

The issue of mismatching time scales comes to a head in the reaction center protein (Fig. 1A). There, a particular set of oscillations exists, which are candidates for excitonic coherences with a lifetime of picoseconds (*13*, *20*). However, excitations in the reaction center transfer away from the participating states within 200 fs (*21*). Because coherences cannot "outlive" populations, an unsettling mismatch between the experimental observation and this fundamental quantum mechanical principle arises (*22*).

RESULTS

We performed 2DES experiments on reaction centers from *Rhodobacter sphaeroides* grown from the carotenoid-deficient R-26 strain (RC_{sph}). The RC_{sph} protein comprises two strongly coupled bacteriochlorophyll*a* molecules (forming a special pair), two accessory bacteriochlorophyll*a*, and two bacteriopheophytin*a* (Fig. 1A). Coupling between these chromophores results in six excitonic states. To enable the use of 2DES at a high laser repetition rate (20 kHz) and to avoid complication of the spectra from charge transfer signals, we used RC_{sph} with a chemically oxidized special pair (P^+). This shortens the photocycle considerably by preventing charge separation, without markedly altering the rate of energy transfer to the special pair (*23*).

The absorption spectrum of the oxidized reaction center at 77 K (Fig. 1B) shows two distinct peaks. The peaks are separated by ~620 cm^{-1} and are associated with the excitonic bands B and H, which have dominant bacteriochlorophyll*a* and bacteriopheophytin*a* contributions, respectively (Fig. 1B). The diagonal peaks in the 2D absorption spectra measured at t_2 = 24 fs match the absorption bands (Fig. 1B).

[1]Department of Chemical Physics, Lund University, Box 124, SE-22100 Lund, Sweden. [2]Department of Chemical Physics, Charles University, Ke Karlovu 3, CZ-121 16 Praha 2, Czech Republic. [3]Department of Chemistry and Molecular Biology, University of Gothenburg, Box 462, SE-40530 Gothenburg, Sweden.
*Present address: Department of Chemistry, University of Zurich, Winterthurerstrasse 190, CH-8057 Zurich, Switzerland.
†Corresponding author. Email: donatas.zigmantas@chemphys.lu.se

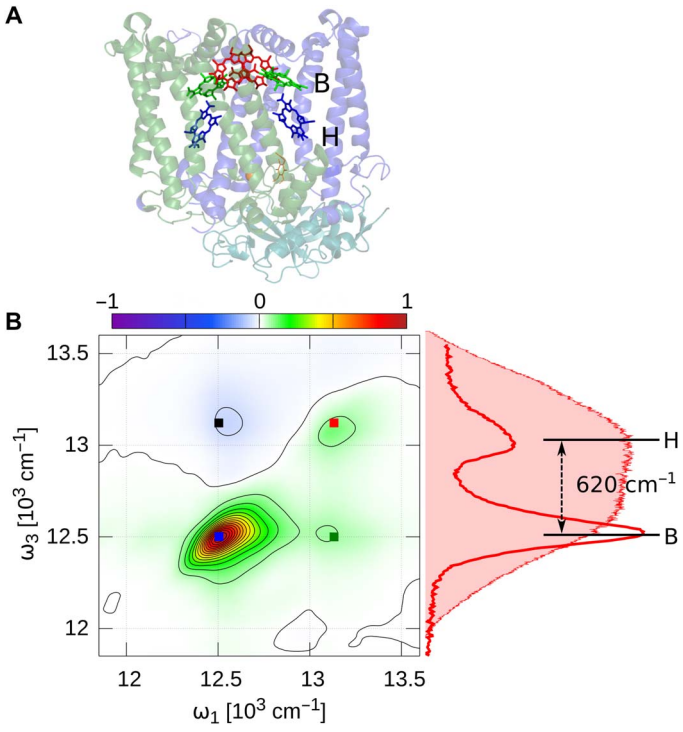

Fig. 1. The structure of RC_{sph}. (**A**) Red, special pair; green, accessory bacteriochlorophylls; blue, bacteriopheophytins. (**B**) The 77-K absorptive 2D spectrum of the oxidized RC_{sph} at t_2 = 24 fs, together with the absorption spectrum and the shaded laser spectrum. The chromophores form a spectroscopic aggregate and give rise to two excitonic absorption bands, which are denoted as B and H. The energy gap between these bands is ~620 cm^{-1}. The absorption of the special pair is absent because of oxidation to P^+.

The positive cross peak below the diagonal indicates coupling and excitation energy transfer between H and B. The negative-valued region above the diagonal arises from the excited-state absorption (ESA) of B. This absorption also masks the upper H-B cross peak. We did not observe distinct features of the two branches of RC_{sph} in the 2DES data.

Features in the 2D spectrum decay or rise monotonously with increasing t_2 and have oscillatory components (*13*). The former reports on the populations of excited states, and the latter indicates coherences.

Picosecond oscillations in RC_{sph} bear all signatures of electronic coherences

The analysis of the coherent beats was performed in three steps. First, we extracted the oscillating residues by subtracting multiexponential fits to real and imaginary parts at each point of the 2D spectrum. Second, the complex-valued residues were Fourier-transformed along t_2. This yields oscillation maps (2D slices of the 3D spectrum), with the positive and negative frequencies $+\omega_2$ and $-\omega_2$, disentangling the system response evolving during the population time t_2, with the phase factor $e^{-i\omega_2 t_2}$ and $e^{+i\omega_2 t_2}$, respectively. This separation is very useful in distinguishing different signal contributions (*15*, *18*). Third, we compare the oscillation maps extracted from all-parallel (polarizations of all laser pulses parallel to each other) and double-cross polarized schemes (relative polarizations of $\pi/4$, $-\pi/4$, $\pi/2$, and 0 for laser pulses 1 to 4). The latter strongly suppresses signals of intramolecular vibrational coherences (produced by the Franck-Condon excitation of vibrational wave packets) (*12*, *13*). All-parallel oscillation maps are presented and discussed in fig. S1 and section S1.

The amplitudes of oscillatory residuals, integrated across the 2D spectra, reveal prominent frequencies of 195, 325, 560, 650, 725, 890, and 1150 cm^{-1} (Fig. 2A, blue line, all-parallel measurement). All of these frequencies can be identified as peaks in the resonance Raman spectra of B (*24*, *25*). The double-cross polarized measurement shows that the amplitudes of the frequencies 195, 325, 725, 890, and 1150 cm^{-1} are suppressed relative to the frequencies at 560 and 650 cm^{-1} (Fig. 2A, red line, double-cross polarized measurement). The sustained frequencies are close to the energy gap between B and H transitions (620 cm^{-1}; see Fig. 1B). This has previously been considered as an indication of an electronic contribution to coherences (*12*, *13*). Furthermore, the double-cross polarized oscillation maps at $\omega_2 = -560$ cm^{-1} and $\omega_2 = +560$ cm^{-1} show off-diagonal peaks (rephasing pulse order) and diagonal peaks (nonrephasing pulse order) (Fig. 2B). A similar pattern is observed for the coherence at $\omega_2 = \pm 650$ cm^{-1} (fig. S2). This pattern is as expected for electronic coherence between the two excitonic states (*17*).

Thus, the coherences at 560 and 650 cm^{-1} for RC_{sph}, if interpreted according to the current understanding of the molecular electronic response, would be concluded to be electronic. However, we determined that the lifetime of the two coherences is longer than 1.6 ps (see fig. S3, table S1, and section S2), which is by an order of magnitude longer than the lifetime of the underlying B and H states. This "lifetime" paradox prompted us to search for an alternative photophysical explanation.

Energy transfer–induced coherence shift offers a comprehensive interpretation for the observed coherences

To resolve this mismatch, we inspect the rephasing oscillation maps at $\omega_2 = 560$ cm^{-1}, measured with the all-parallel pulse sequence (Fig. 3A). The general pattern of the map computed from the complex-valued data matches a combination of vibrational coherences in the excited-state [stimulated emission (SE)] and ground-state [ground-state bleach (GSB)] pathways (Fig. 3B, fig. S4, and section S3). We do not consider ESA here because of its small contribution (see Fig. 1B). Note that when computing the oscillation map from real-valued data, a cancellation of the signal on the diagonal B peak appears (Fig. 3A). However, this is inconsistent with a sum of the SE and GSB pathways, which have the same sign and therefore would interfere constructively mostly on the diagonal (see section S3 for details). Additionally, the data for $t_2 < 216$ fs were omitted from our computation of oscillation maps, and thus, the SE signal is expected to be negligible. This is because the energy transfer from B to P^+ is mostly completed after 216 fs.

We therefore propose that all coherences observed in oscillation maps (Fig. 3) are in the ground state. For the SE-like pathways, the first two laser pulses create a coherence that either is purely vibrational in the B excited state or has a mixed vibronic origin, involving B and H states (*26*). Then, the coherence is shifted to the ground state. Here, vibrational wave packets can live for several picoseconds, independent of the excited-state lifetime. The shift of coherence is the key component of our mechanism. We propose that it is induced by the ultrafast energy transfer from B to P^+ (*27*), and we therefore term this process as *energy transfer–induced coherence shift* (ETICS) (schematically shown in Fig. 4A). Note that it is different from canonical coherence transfer, where one superposition of states is transferred to a different superposition of states without substantial energy dissipation.

ETICS response pathways presented in Fig. 3 show that they should produce signals that have an opposite sign (π-phase shift) compared to the corresponding signals from SE pathways (fig. S4) (*27*). The zero

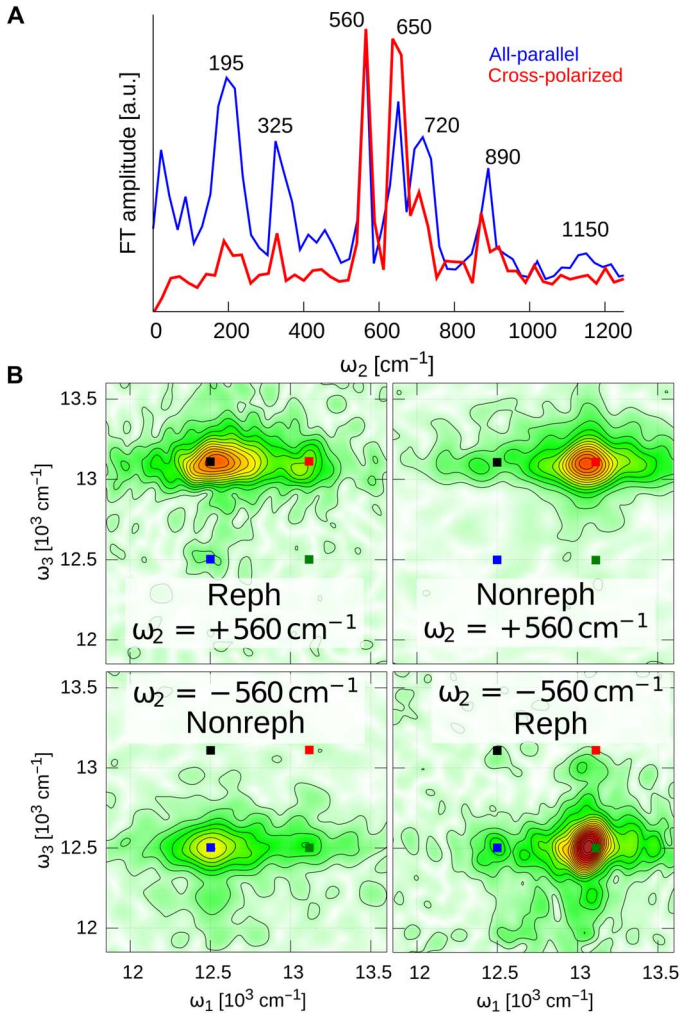

Fig. 2. Suppression of the intramolecular vibrational coherences by the polarization-resolved 2DES. (**A**) The amplitude of integrated oscillation maps over ω_1 and ω_3 show all the beating frequencies present in the all-parallel and double-cross polarized measurements. The relative enhancement of the modes with frequencies $\omega_2 = 560$ and 650 cm^{-1} close to the excitonic splitting between B and H is clearly visible in the double-cross polarized experiment. The spectra are normalized at 560 cm^{-1}. FT, Fourier transform; a.u., arbitrary units. (**B**) $\omega_2 = \pm 560$ cm^{-1} oscillation maps, extracted from the double-cross polarized spectra, measured between 216 and 1620 fs. The rephasing (Reph) part oscillates exclusively off-diagonal, and the nonrephasing (Nonreph) part oscillates on-diagonal only. The sign of the ω_2 frequency indicates the phase evolution direction in the complex plane. All the features of the presented maps point (misleadingly) to the electronic origin of the beatings. The colored squares depict positions of the main peaks in the 2D spectrum.

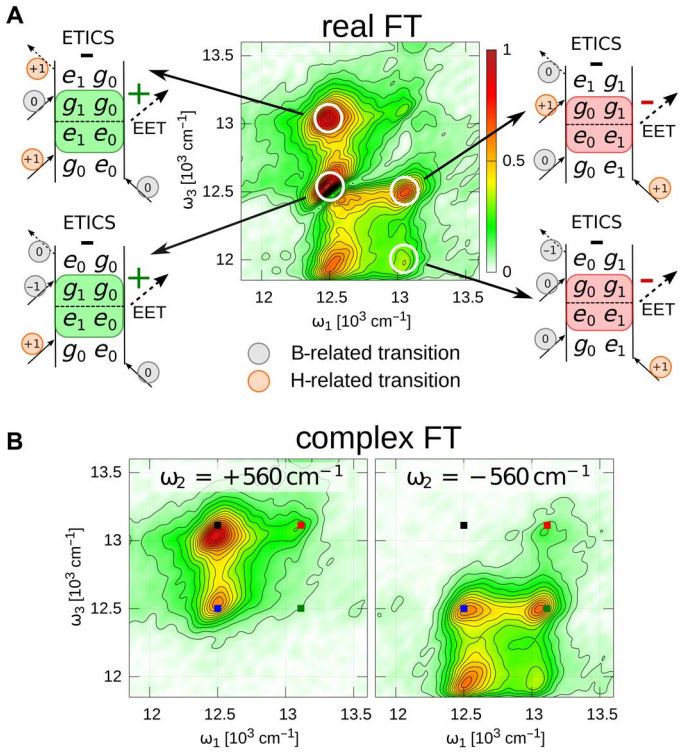

Fig. 3. Cancellation of the signals at the diagonal peak 12,500 cm^{-1} in the all-parallel measurement reveals the ETICS phenomenon. (**A**) The $\omega_2 = 560$ cm^{-1} oscillation map, computed from real-valued rephasing spectra measured between $t_2 = 216$ and 1740 fs. The associated Feynman diagrams show all the rephasing ETICS pathways, which are complementary to their SE analogs (fig. S4). *g* and *e* denote the ground and electronically excited states; the subscript indicates the vibrational quantum number. Mixing between e_1 of B and e_0 of H states is implied whenever e_1 appears in the diagrams. The number next to each transition arrow indicates the change of the vibrational quantum number. The transition in the shaded parts of the diagrams corresponds to the energy transfer with the indicated ω_2 sign next to them. The contribution sign of ETICS signals is opposite to the SE analogs and is shown above each diagram. EET, electronic energy transfer. (**B**) The decomposition of the oscillation map shown in (A) to $\pm\omega_2$ frequency maps by computing the Fourier transform of the complex-valued data shows two distinct contributions to the diagonal. Constructive interference would be observed on the diagonal between SE ($+\omega_2$) and GSB ($-\omega_2$) signals (fig. S4). However, the ETICS process changes the sign of the SE analog, resulting in the observed cancellation.

signal node in the B diagonal (Fig. 3A) is then readily explained, because the GSB pathways and ETICS pathways overlap and cancel out. The absence of total cancellation is accounted for by the opposite phase sweep across the oscillation peaks in the GSB and ETICS signals (see section S3). The inclusion of the ETICS pathways also agrees with the observed relative amplitudes of the peaks in the oscillation maps in Fig. 3 (see section S3 for details). Notably, we find the nodal line in other oscillation frequency maps as well, which is consistent with the ETICS process, as it should occur for all vibrational wave packets (figs. S1 and S2).

In ETICS, the SE coherence shifts to the ground state within ~200 fs, which should result in a π-phase shift in the oscillatory signal. This behavior should be observable at a spectral position, which is clear of the GSB oscillation signals from impulsive Raman scattering (*28*). Therefore, we search for the phase flip in the kinetic trace of the upper cross peak in the rephasing double-cross polarized measurement (Fig. 4, B and C), where only one ETICS pathway contributes. The real and imaginary oscillating residuals are fitted simultaneously in the time window t_2 = 216 to 1620 fs to a sum of two complex exponentials, which account for the two frequencies at 560 and 650 cm^{-1}. The fits are then extrapolated to $t_2 = 0$. Indeed, a π-phase shift is observed in the absorptive (real) and refractive (imaginary) part of the signal during the characteristic time of the energy transfer from B to P^+ (see Fig. 4). The agreement with the expected behavior for ETICS is excellent, especially when considering that the initial oscillating signal up to t_2 = 216 fs can contain different contributions, including an electronic H-B coherence.

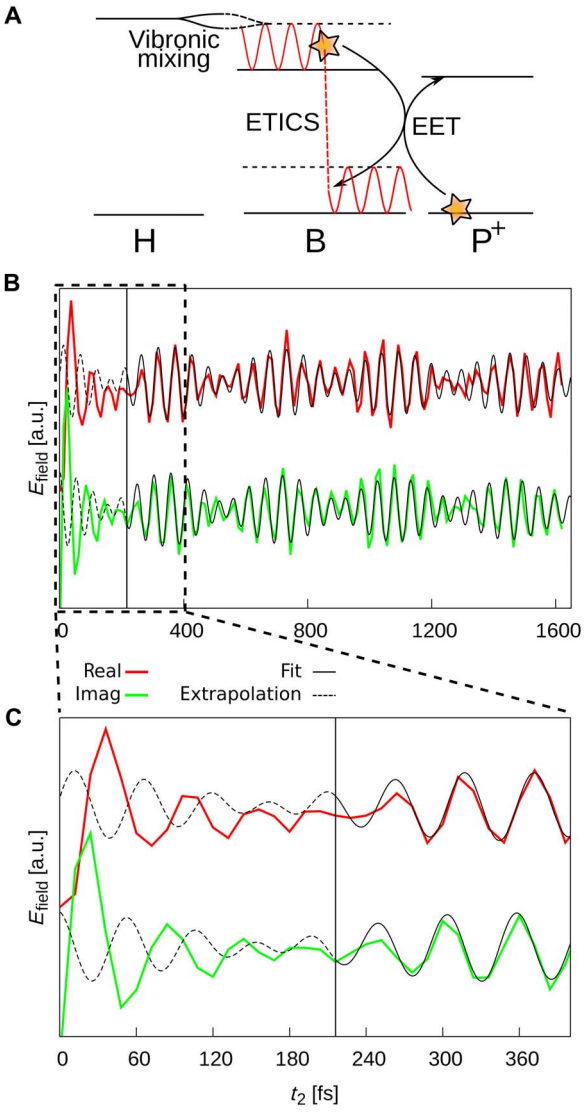

Fig. 4. The ETICS process observed in the time domain. (**A**) Scheme of the ETICS process showing how initially created excited-state coherence is shifted to the ground state during the energy transfer step to P^+. Vibronic mixing between bacteriochlorophyll and bacteriopheophytin states leads to the observable beating signals in the double-cross polarized measurement for vibrational frequencies close to the B-H electronic gap. Observation of ETICS identifies a hot energy transfer pathway where the access energy is damped in the donor ground state on the picosecond time scale. (**B**) Evolution of the real (red) and imaginary (green) parts of the upper cross peak in the rephasing double-cross polarized measurement and a fit by the sum of two complex exponentials (black) for $t_2 > 216$ fs. Extrapolation of the fit to $t_2 = 0$ fs (dashed line) demonstrates a π-phase change, as compared to the later population times. (**C**) Zoom-in into the first 400 fs of the population time.

DISCUSSION

How general is the ETICS phenomenon? One strict requirement is that energy transfer occurs during vibrational cooling. Another requirement is that the vibrational modes on the ground and excited electronic states are similar. Both requirements are often fulfilled in photosynthetic proteins, including reaction centers and light-harvesting complexes. Thus, ETICS can be expected to be general.

ETICS retains exactly the same beating patterns as the corresponding SE pathways. Therefore, its spectral signatures can be easily misinterpreted as long-lived coherences with electronic character (*13*). For example, the oscillation maps of a plant reaction center protein by Fuller *et al.* (*29*) show that the signal on the diagonal line cancels, which is not reproduced by the model proposed in their study but could be explained by the ETICS process.

Moreover, the hypothesis that energy transport in photosynthetic proteins is wavelike rests on the assignment of coherences to the superposition of excitonic states (*6*, *12*, *19*). ETICS provides an alternative assignment of the coherences and therefore calls for reconsideration of the wavelike energy transfer. Clearly, a careful analysis of beatings in other photosynthetic proteins is needed for an accurate designation of contributing photophysical phenomena.

Vibronic mixing in RC_{sph}

Finally, we clarify why long-lived coherences with certain frequencies (that is, 560 and 650 cm^{-1}) are observed in the double-cross polarized measurement, although this pulse sequence excludes all vibrational coherences generated by the intramolecular Franck-Condon excitations (*12*, *13*). This is revealed by the signals in the oscillation maps for $\omega_2 = \pm 560$ cm^{-1} (Fig. 2B; for $\omega_2 = \pm 650$ cm^{-1}, see fig. S2). We find that the observed oscillation patterns for the double-cross polarized pulse sequence (Fig. 2B) match well with only two ETICS pathways in the rephasing signal (see the Supplementary Materials for a detailed pathway analysis). These pathways can only contribute to the signal if the two transitions $g_0 \rightarrow e_0$ and $g_0 \rightarrow e_1$ (see Feynman diagrams in Fig. 3A) have nonparallel transition dipole moments. Thus, the initially excited states in the RC_{sph} aggregate must be vibronically coupled, that is, state e_1 consists of the nonadiabatic mixture of the vibronically excited state of accessory bacteriochlorophyll and the electronically excited state of bacteriopheophytin. This implies that vibrations are at least partly delocalized between accessory bacteriochlorophyll and bacteriopheophytin. Thus, we find that vibronic mixing occurs in RC_{sph} and that it is essential for the observation of ETICS pathways in the double-cross polarized measurement. However, in general, vibronic mixing is not necessary for ETICS to occur. This is supported by the observation of the ETICS phenomenon for vibrational modes, which are out of resonance with the H-B excitonic gap and therefore are not mixed (see fig. S1).

Vibronic mixing has recently been suggested for natural (*26*, *28*, *30*, *31*) and synthetic (*14*) light-harvesting complexes. It has been proposed to facilitate energy transfer (*28*, *30*, *32*), and it has also been used to explain long-lived quantum coherences (*22*, *26*, *28*, *29*, *33*, *34*). In particular, Christensson *et al.* (*26*) predicted that the mixing of nuclear and electronic degrees of freedom leads to the slow dephasing of mixed vibronic coherences in the excited state. However, because the lifetime of the excited states is shorter than 200 fs, we do not consider this hypothesis a viable explanation for the long-lived beatings in RC_{sph}.

Tiwari *et al.* (*28*) proposed that vibronic coupling of the excited states opens up a new response pathway by which direct excitation of ground-state vibrational coherences is facilitated. This model was used to interpret the long-lived oscillating signals observed in the two-color photon echo experiments of RC_{sph} (*22*). However, we do not find the predicted strong asymmetry of oscillation amplitudes in the cross peaks above and below the diagonal in the 2D spectra (see Fig. 2B and section S4 for details). Moreover, the pathways suggested in the study of Tiwari *et al.* (*28*) are inconsistent with the phase shift that we observed on the 200-fs time scale (Fig. 4), leading to cancellation of the oscillating signals appearing on the diagonal B peak in the all-parallel measurement (Fig. 3A). Thus, we conclude that direct excitation of ground-state vibrational coherence, as proposed by Tiwari *et al.* (*28*), is not dominant in RC_{sph}.

Hot energy transfer in RC_{sph} facilitated by vibrational dissipation in the ground state

Although we observe ETICS as a shift of vibrational coherences between electronic states, equivalent "shift" of populations, which include energy transfer from vibronically hot state, are equally possible. This indicates an energy transfer channel from hot B to the special pair, whereas a vibrational quantum is left on the accessory bacteriochlorophyll. Thus, the vibrational modes on the accessory bacteriochlorophylls work as a sink by taking up the excess energy from the energy transfer between B and the special pair. Here, we show that many vibrational modes on accessory bacteriochlorophylls can act as an energy sink for the energy transfer step (*35*). Energy conversion demands the existence of these modes, but it has not been possible to spectroscopically detect them. Our finding opens a new possibility of following the dissipation of excess energy in excitation transfer into vibrations of the molecules.

We identified the special modes that have frequencies close to the B-H resonance. They have a twofold effect on energy transfer. First, vibronic mixing increases the rate of energy transfer between B and H (*28*, *30*), leading to the efficient population of hot B. Second, these modes can accelerate energy transfer further from hot B to the special pair, before vibrational relaxation on B takes place on a picosecond time scale. As seen from a molecular perspective, the atoms of the chromophore are already set to oscillate within an appropriate mode in the excited state, priming the molecules for energy transfer. Thus, certain modes appear to be an integral part of downhill energy transfer, increasing its overall efficiency. The availability of these special modes of chromophores may explain the extraordinarily fast energy transfer rates in reaction center proteins. Also, the possibility that the protein uses these modes to control the directionality of the flow of energy should not be disregarded.

MATERIALS AND METHODS

Reaction centers

Reaction centers were isolated from *R. sphaeroides*, R-26, following standard procedures described elsewhere (*36*), with modifications described in section S5. To oxidize RC_{sph}, potassium ferricyanide $[K_3Fe(CN)_6]$ was added to a final concentration of 150 mM. Samples were mixed with glycerol at the 35:65 (v/v) ratio and cooled down to 77 K in a 0.5 mm cell made of fused silica. The samples typically had an optical density (OD) of 0.2 to 0.3 at 800 nm.

Spectroscopy setup

The data acquisition protocol and the analysis were described previously (*37*–*39*). Briefly, a noncollinear optical amplifier was pumped by the 1030 nm fundamental output of the PHAROS laser system (Light Conversion Ltd.). The resulting ~17 fs laser pulses were split into four beams using a beam splitter and a transmissive diffraction grating. Spherical optics were used to focus all beams to ~160 μm on the sample spot. One of the beams was attenuated by a neutral density filter with an OD of 2 and used as local oscillator for the heterodyne detection. The first two beams were simultaneously chopped by mechanical choppers, and a double frequency lock-in detection scheme was used. Interferograms were continuously detected by a CCD (PIXIS, Princeton Instruments).

A repetition rate of 20 kHz with excitation energies of 2 and 4 nJ per pulse was used for all-parallel and double-cross polarized measurements, respectively. This translates to an excitation density of 4×10^{13} photons per pulse per cm^2 for the 2 nJ pulse energy. The population time step was 12 fs, which defines the high-frequency cutoff to $\omega_2 = 1389\ cm^{-1}$. The coherence time t_1 was scanned from −199.5 to 294 fs (−171.5 to 273 fs), with the 1.75 fs step for all-parallel (double-cross polarized) measurements. In both axes, the resolution was typically 50 cm^{-1} (58 cm^{-1}) for the all-parallel (double-cross polarized) experiments (section S5).

Data handling

The sequences of 2D spectra in t_2 were Fourier-transformed to generate 3D Fourier transform spectra. To reduce the complexity of the third-order response signals and to avoid multiple resonant and nonresonant contributions during the pulse overlap, we analyzed the oscillating signals in the following way. We extracted the oscillatory components in t_2 by subtracting multiexponential fits with complex amplitude prefactors from each (ω_1, ω_3) data point. The Fourier transform of the remaining oscillating residuals in t_2 yielded the 3D Fourier transform spectra. By slicing these spectra in ω_2, we extracted the (ω_1, ω_3) oscillation maps for each ω_2 frequency. The resolution along ω_2 is determined by the length of the t_2 scan, which was 0 to 1740 fs and 0 to 1620 fs, resulting in frequency resolution of 22 and 24 cm^{-1} for all-parallel and double-cross polarized measurements, respectively.

SUPPLEMENTARY MATERIALS

Supplementary material for this article is available at http://advances.sciencemag.org/cgi/content/full/3/9/e1603141/DC1

section S1. Oscillation maps
section S2. Direct observation of the phase shift in the time domain
section S3. Analysis of the interaction pathways
section S4. Vibronic coupling
section S5. Experimental methods
fig. S1. Oscillation maps of coherences with the indicated frequencies.
fig. S2. Comparison of the oscillation maps in all-parallel and double-cross polarized measurements.
fig. S3. Time-domain coherent oscillation traces.
fig. S4. Interaction pathway analysis.
table S1. Fitting parameters of the rephasing time-domain traces at the B-H cross peak.
References (*40*–*43*)

REFERENCES AND NOTES

1. M. H. Vos, M. R. Jones, C. N. Hunter, J. Breton, J.-C. Lambry, J.-L. Martin, Coherent dynamics during the primary electron-transfer reaction in membrane-bound reaction centers of *Rhodobacter sphaeroides*. *Biochemistry* **33**, 6750–6757 (1994).
2. S. Savikhin, Y. Zhu, S. Lin, R. E. Blankenship, W. S. Struve, Femtosecond spectroscopy of chlorosome antennas from the green photosynthetic bacterium *Chloroflexus aurantiacus*. *J. Phys. Chem.* **98**, 10322–10334 (1994).
3. D. C. Arnett, C. C. Moser, P. L. Dutton, N. F. Scherer, The first events in photosynthesis: Electronic coupling and energy transfer dynamics in the photosynthetic reaction center from *Rhodobacter sphaeroides*. *J. Phys. Chem. B* **103**, 2014–2032 (1999).
4. S. Savikhin, D. R. Buck, W. S. Struve, Oscillating anisotropies in a bacteriochlorophyll protein: Evidence for quantum beating between exciton levels. *Chem. Phys.* **223**, 303–312 (1997).
5. D. M. Jonas, Two-dimensional femtosecond spectroscopy. *Annu. Rev. Phys. Chem.* **54**, 425–463 (2003).
6. G. S. Engel, T. R. Calhoun, E. L. Read, T.-K. Ahn, T. Mančal, Y.-C. Cheng, R. E. Blankenship, G. R. Fleming, Evidence for wavelike energy transfer through quantum coherence in photosynthetic systems. *Nature* **446**, 782–786 (2007).
7. A. Nemeth, F. Milota, T. Mančal, V. Lukeš, H. F. Kauffmann, J. Sperling, Vibronic modulation of lineshapes in two-dimensional electronic spectra. *Chem. Phys. Lett.* **459**, 94–99 (2008).
8. T. Brixner, J. Stenger, H. M. Vaswani, M. Cho, R. E. Blankenship, G. R. Fleming, Two-dimensional spectroscopy of electronic couplings in photosynthesis. *Nature* **434**, 625–628 (2005).
9. D. Zigmantas, E. L. Read, T. Mančal, T. Brixner, A. T. Gardiner, R. J. Cogdell, G. R. Fleming, Two-dimensional electronic spectroscopy of the B800–B820 light-harvesting complex. *Proc. Natl. Acad. Sci. U.S.A.* **103**, 12672–12677 (2006).

10. E. Thyrhaug, K. Žídek, J. Dostál, D. Bína, D. Zigmantas, Exciton structure and energy transfer in the Fenna–Matthews–Olson complex. *J. Phys. Chem. Lett.* **7**, 1653–1660 (2016).
11. R. M. Hochstrasser, Two-dimensional IR-spectroscopy: Polarization anisotropy effects. *Chem. Phys.* **266**, 273–284 (2001).
12. G. S. Schlau-Cohen, A. Ishizaki, T. R. Calhoun, N. S. Ginsberg, M. Ballottari, R. Bassi, G. R. Fleming, Elucidation of the timescales and origins of quantum electronic coherence in LHCII. *Nat. Chem.* **4**, 389–395 (2012).
13. S. Westenhoff, D. Paleček, P. Edlund, P. Smith, D. Zigmantas, Coherent picosecond exciton dynamics in a photosynthetic reaction center. *J. Am. Chem. Soc.* **134**, 16484–16487 (2012).
14. J. Lim, D. Paleček, F. Caycedo-Soler, C. N. Lincoln, J. Prior, H. von Berlepsch, S. F. Huelga, M. B. Plenio, D. Zigmantas, J. Hauer, Vibronic origin of long-lived coherence in an artificial molecular light harvester. *Nat. Commun.* **6**, 7755 (2015).
15. H. Li, A. D. Bristow, M. E. Siemens, G. Moody, S. T. Cundiff, Unraveling quantum pathways using optical 3D Fourier-transform spectroscopy. *Nat. Commun.* **4**, 1390 (2013).
16. F. Milota, V. I. Prokhorenko, T. Mancal, H. von Berlepsch, O. Bixner, H. F. Kauffmann, J. Hauer, Vibronic and vibrational coherences in two-dimensional electronic spectra of supramolecular J-aggregates. *J. Phys. Chem. A* **117**, 6007–6014 (2013).
17. V. Butkus, D. Zigmantas, L. Valkunas, D. Abramavicius, Vibrational vs. electronic coherences in 2D spectrum of molecular systems. *Chem. Phys. Lett.* **545**, 40–43 (2012).
18. J. Seibt, T. Hansen, T. Pullerits, 3D spectroscopy of vibrational coherences in quantum dots: Theory. *J. Phys. Chem. B* **117**, 11124–11133 (2013).
19. E. Collini, C. Y. Wong, K. E. Wilk, P. M. G. Curmi, P. Brumer, G. D. Scholes, Coherently wired light-harvesting in photosynthetic marine algae at ambient temperature. *Nature* **463**, 644–647 (2010).
20. H. Lee, Y.-C. Cheng, G. R. Fleming, Coherence dynamics in photosynthesis: Protein protection of excitonic coherence. *Science* **316**, 1462–1465 (2007).
21. D. M. Jonas, M. J. Lang, Y. Nagasawa, T. Joo, G. R. Fleming, Pump–probe polarization anisotropy study of femtosecond energy transfer within the photosynthetic reaction center of *Rhodobacter sphaeroides* R26. *J. Phys. Chem.* **100**,12660–12673 (1996).
22. I. S. Ryu, H. Dong, G. R. Fleming, Role of electronic-vibrational mixing in enhancing vibrational coherences in the ground electronic states of photosynthetic bacterial reaction center. *J. Phys. Chem. B* **118**, 1381–1388 (2014).
23. J. A. Jackson, S. Lin, A. K. W. Taguchi, J. C. Williams, J. P. Allen, N. W. Woodbury, Energy transfer in *Rhodobacter sphaeroides* reaction centers with the initial electron donor oxidized or missing. *J. Phys. Chem. B* **101**, 5747–5754 (1997).
24. N. J. Cherepy, A. P. Shreve, L. J. Moore, S. G. Boxer, R. A. Mathies, Temperature dependence of the Q_y resonance Raman spectra of bacteriochlorophylls, the primary electron donor, and bacteriopheophytins in the bacterial photosynthetic reaction center. *Biochemistry* **36**, 8559–8566 (1997).
25. K. Czarnecki, J. R. Diers, V. Chynwat, J. P. Erickson, H. A. Frank, D. F. Bocian, Characterization of the strongly coupled, low-frequency vibrational modes of the special pair of photosynthetic reaction centers via isotopic labeling of the cofactors. *J. Am. Chem. Soc.* **119**, 415–426 (1997).
26. N. Christensson, H. F. Kauffmann, T. Pullerits, T. Mančal, Origin of long-lived coherences in light-harvesting complexes. *J. Phys. Chem. B* **116**, 7449–7454 (2012).
27. T. Mančal, J. Dostál, J. Pšenčík, D. Zigmantas, Transfer of vibrational coherence through incoherent energy transfer process in Förster limit. *Can. J. Chem.* **92**, 135–143 (2014).
28. V. Tiwari, W. K. Peters, D. M. Jonas, Electronic resonance with anticorrelated pigment vibrations drives photosynthetic energy transfer outside the adiabatic framework. *Proc. Natl. Acad. Sci. U.S.A.* **110**, 1203–1208 (2013).
29. F. D. Fuller, J. Pan, A. Gelzinis, V. Butkus, S. S. Senlik, D. E. Wilcox, C. F. Yocum, L. Valkunas, D. Abramavicius, J. P. Ogilvie, Vibronic coherence in oxygenic photosynthesis. *Nat. Chem.* **6**, 706–711 (2014).
30. J. M. Womick, A. M. Moran, Vibronic enhancement of exciton sizes and energy transport in photosynthetic complexes. *J. Phys. Chem. B* **115**, 1347–1356 (2011).
31. A. W. Chin, J. Prior, R. Rosenbach, F. Caycedo-Soler, S. F. Huelga, M. B. Plenio, The role of non-equilibrium vibrational structures in electronic coherence and recoherence in pigment–protein complexes. *Nat. Phys.* **9**, 113–118 (2013).
32. V. Perlík, J. Seibt, L. J. Cranston, R. J. Cogdell, C. N. Lincoln, J. Savolainen, F. Šanda, T. Mančal, J. Hauer, Vibronic coupling explains the ultrafast carotenoid-to-bacteriochlorophyll energy transfer in natural and artificial light harvesters. *J. Chem. Phys.* **142**, 212434 (2015).
33. M. Ferretti, V. I. Novoderezhkin, E. Romero, R. Augulis, A. Pandit, D. Zigmantas, R. van Grondelle, The nature of coherences in the B820 bacteriochlorophyll dimer revealed by two-dimensional electronic spectroscopy. *Phys. Chem. Chem. Phys.* **16**, 9930–9939 (2014).
34. E. Romero, R. Augulis, V. I. Novoderezhkin, M. Ferretti, J. Thieme, D. Zigmantas, R. van Grondelle, Quantum coherence in photosynthesis for efficient solar-energy conversion. *Nat. Phys.* **10**, 676–682 (2014).
35. J. Schulze, M. F. Shibl, M. J. Al-Marri, O. Kühn, Multi-layer multi-configuration time-dependent Hartree (ML-MCTDH) approach to the correlated exciton-vibrational dynamics in the FMO complex. *J. Chem. Phys.* **144**, 185101 (2016).
36. R. Farhoosh, V. Chynwat, R. Gebhard, J. Lugtenburg, H. A. Frank, Triplet energy transfer between the primary donor and carotenoids in *Rhodobacter sphaeroides* R-26.1 reaction centers incorporated with spheroidene analogs having different extents of π-electron conjugation. *Photochem. Photobiol.* **66**, 97–104 (1997).
37. T. Brixner, T. Mančal, I. V. Stiopkin, G. R. Fleming, Phase-stabilized two-dimensional electronic spectroscopy. *J. Chem. Phys.* **121**, 4221–4236 (2004).
38. R. Augulis, D. Zigmantas, Two-dimensional electronic spectroscopy with double modulation lock-in detection: Enhancement of sensitivity and noise resistance. *Opt. Express* **19**, 13126–13133 (2011).
39. R. Augulis, D. Zigmantas, Detector and dispersive delay calibration issues in broadband 2D electronic spectroscopy. *J. Opt. Soc. Am. B* **30**, 1770–1774 (2013).
40. D. Paleček, Quantum coherence for light harvesting, thesis, Lund University (2015).
41. M. Rätsep, Z.-L. Cai, J. R. Reimers, A. Freiberg, Demonstration and interpretation of significant asymmetry in the low-resolution and high-resolution Q_y fluorescence and absorption spectra of bacteriochlorophyll *a*. *J. Chem. Phys.* **134**, 024506 (2011).
42. S. Mukamel, *Principles of Nonlinear Optical Spectroscopy* (Oxford Univ. Press, 1995).
43. F. Milota, C. N. Lincoln, J. Hauer, Precise phasing of 2D-electronic spectra in a fully non-collinear phase-matching geometry. *Opt. Express* **21**, 15904–15911 (2013).

Acknowledgments: We would like to thank D. Abramavicius, V. Butkus, L. Valkunas, T. Pullerits, and T. Mančal for helpful discussions. **Funding:** The work in Lund was supported by the Swedish Research Council and the Knut and Alice Wallenberg Foundation. S.W. and P.E. acknowledge funding from the Swedish Foundation for Strategic Research, the Olle Engkvist Byggmästare Foundation, and the Swedish Research Council. **Author contributions:** D.P., S.W., and D.Z. conceived and designed the experiments. D.P. performed the experiments. D.P. analyzed the data. P.E. grew and purified the samples. D.P., D.Z., S.W., and P.E. wrote the manuscript. All authors discussed the results and commented on the manuscript. **Competing interests:** The authors declare that they have no competing interests. **Data and materials availability:** All data needed to evaluate the conclusions in the paper are present in the paper and/or the Supplementary Materials. Additional data related to this paper may be requested from the authors.

Submitted 20 December 2016
Accepted 8 August 2017
Published 6 September 2017
10.1126/sciadv.1603141

Citation: D. Paleček, P. Edlund, S. Westenhoff, D. Zigmantas, Quantum coherence as a witness of vibronically hot energy transfer in bacterial reaction center. *Sci. Adv.* **3**, e1603141 (2017).

Quantum coherence as a witness of vibronically hot energy transfer in bacterial reaction center

David Palecek, Petra Edlund, Sebastian Westenhoff and Donatas Zigmantas

Sci Adv **3** (9), e1603141.
DOI: 10.1126/sciadv.1603141